Title	F spots and domain patterns in rhombohedral PbZr0.90Ti0.10O3
Author(s)	Huang, Haitao; Zhou, Li Min; Guo, Jun; Hng, Huey Hoon; Oh, Joo Tien; Hing, Peter
Citation	Huang, H., Zhou, L. M., Guo, J., Hng, H. H., Oh, J. T., & Hing, P. (2003). F spots and domain patterns in rhombohedral PbZr0.90Ti0.10O3. Applied physics letters, 83(18), 3692-3694.
Date	2003
URL	http://hdl.handle.net/10220/18839
Rights	

F spots and domain patterns in rhombohedral $PbZr_{0.90}Ti_{0.10}O_3$

Haitao Huang[a] and Li Min Zhou
Department of Mechanical Engineering, The Hong Kong Polytechnic University, Hung Hom, Kowloon, Hong Kong

Jun Guo, Huey Hoon Hng, Joo Tien Oh, and Peter Hing
School of Materials Engineering, Nanyang Technological University, Singapore 639798

(Received 24 June 2003; accepted 12 September 2003)

The microstructure of $PbZr_{0.9}Ti_{0.1}O_3$ ceramics is studied by transmission electron microscopy. Two types of domain patterns are found, namely, the 109° domain with the *F* spots ($\frac{1}{2}\{hkl\}$ superlattice reflections) observed in neighboring domains and the 71° domain with the *F* spots observed in one domain and having disappeared in the neighboring one. The computer simulation indicates that the *F* spots are forbidden at $h=k$ positions so that they do not appear in the electron diffraction pattern if viewed along the $[\bar{1}10]$ direction. Based on this result, the observed two types of domain patterns and their corresponding diffraction patterns can be explained. © *2003 American Institute of Physics.* [DOI: 10.1063/1.1624632]

The solid solution of the $PbZrO_3-PbTiO_3$ (PZT) system has been extensively studied for its interesting technical properties like pyro- and piezoelectricity. It displays a complex phase diagram.[1] At room temperature, depending on the Zr/Ti ratio, it shows the antiferroelectric orthorhombic phase A_O, two ferroelectric rhombohedral phases ($F_{R(\mathrm{HT})}$ and $F_{R(\mathrm{LT})}$), the tetragonal phase F_T, and a new monoclinic phase between $F_{R(\mathrm{HT})}$ and F_T.[2] The Zr-rich rhombohedral phase has important pyroelectric applications due to its strong temperature dependence of the spontaneous polarization and relatively low dielectric constant.[3–5] There have been many studies focused on the structure of Zr-rich rhombohedral phase. It is generally agreed that at room temperature the rhombohedral $F_{R(\mathrm{LT})}$ phase has the space group $R3c$ and exhibits both a cation shift along the pseudocubic [111] direction and oxygen octahedra tilting around [111].[6] The oxygen octahedra tilting results from the condensation of optical phonon modes, either at the *R* or *M* point of the Brillouin zone boundary.[7] As the temperature increases, the tilting of the oxygen octahedra is gradually decreased to zero, leading to a phase transition to $F_{R(\mathrm{HT})}$. However, the cation shift still remains and the ferroelectric phase is kept up to the Curie temperature until a final phase transition to the paraelectric cubic phase.

Many electron diffraction studies have already shown that the existence of the $\frac{1}{2}\{hkl\}$ (the so-called *F* spots) superlattice reflections is closely related to antiphase octahedra tilting.[7–15] Since the oxygen octahedra are corner linked throughout the perovskite lattice, they form a relatively rigid framework. Thus, the tilting of one octahedron around the principle axis will cause the antiparallel tilting of all the neighboring octahedra lying in the same plane perpendicular to that axis. This doubles the unit cell in that plane. However, the origin of the superlattice reflections is not fully understood and disputes still remain. Glazer[16] has shown that antiphase oxygen octahedra tilting will generate $\frac{1}{2}\{hkl\}$ type of superlattice reflections except that reflections at $h=k=l$ are forbidden, which has been proved by neutron diffraction studies.[9] Dynamical effects have been proposed to be responsible for the appearance of these $h=k=l$ type of *F* spots in electron diffraction patterns.[13] Computer simulations, however, have shown that octahedral tilts and distortions alone are insufficient to give rise to *R*-type superlattice reflections with the intensities observed.[9] Antiparallel displacements of the Pb ions have been postulated by Ricote *et al.*[9] to account for the observed intensities. Shortly after, the model was modified by the same group,[17] according to a more accurate data from neutron diffraction. They have introduced alternative shifts of Pb ions along the [100] and [010] directions. Although the domain configuration of rhombohedral PZT ceramics has also been studied before,[18,19] the relationship between the domain pattern and *F* spots is not fully studied. From computer simulation, we found that due to the tilting of octahedra and the shifting of Pb ions, the electron diffraction pattern is no longer identical for various ⟨110⟩-type zone axes. The *F* spots disappear in the electron diffraction pattern if viewed along $[\bar{1}10]$. In this letter, we will report experimental evidence that the *F* spots are not always observed for different types of domains.

The material used in the present study is $Pb(Zr_{0.90}Ti_{0.10})O_3$ ceramics. It was prepared through the conventional solid state reaction of mixed-oxide powders. The detailed procedure for materials processing and transmission electron microscopy (TEM) sample preparation can be found elsewhere.[5,8] The TEM studies were conducted on a 200 kV JEOL JEM-2010 microscope on a double-tilt stage.

Figure 1 shows the typical wedge-shaped domain pattern viewed along $[\bar{1}01]$. The insert is a selected area diffraction pattern (SADP) with a zone axis of $[\bar{1}01]$. The *F* spots can be clearly seen, as indicated by an arrow. The two neighboring domains A and B have similar SADPs and both of them have the *F* spots. The domain walls are oriented along the $(\bar{1}10)$ plane, which cuts through the paper plane $(\bar{1}01)$ along the $[\bar{1}1\bar{1}]$ direction. It is known that for rhombohedral PZT, there are three types of domain boundaries: 109°, 71°, and

[a]Author to whom correspondence should be addressed; electronic mail: mmhhuang@polyu.edu.hk

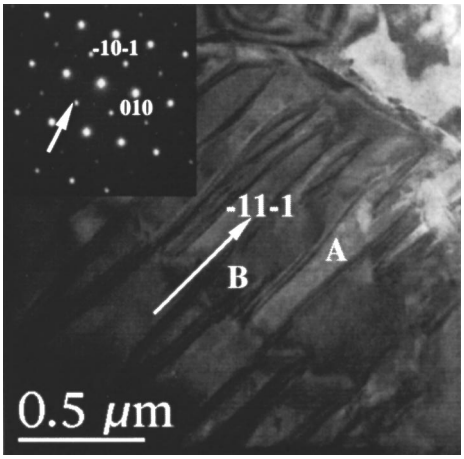

FIG. 1. 109° domain pattern viewed along $[\bar{1}01]$. Inset shows a SADP pattern (*F*-spot is indicated by an arrow).

180°. The orientations of the permissible uncharged walls are {110} for 109°, {001} for 71°, and any plane parallel to the polarization vector (along the [111] direction) for 180° domains.[18] It has been reported that the surface energy of a {100}-type domain boundary is three times that of a {110}-type one.[19] Therefore, the 109° domains, as shown in Fig. 1, are the most frequently observed under TEM. The (110) wall is not parallel to the electron beam so that a diffraction contrast pattern of fringes, i.e., the closely spaced parallel lines along the $[\bar{1}1\bar{1}]$ direction, can be seen in Fig. 1.

Figure 2 shows a less commonly observed 71° domain pattern viewed along $[\bar{1}01]$. The insets are the SADPs of two neighboring domains labeled A and B. The domain wall between A and B is identified as the (010) plane. This wall is parallel to the electron beam so that no similar fringe patterns, as shown in Fig. 1, can be seen. *F* spots (as indicated by an arrow) can only be found from the SADP of domain A. No *F* spots are found on the SADP of domain B. We have reported the alternative appearance and disappearance of the *F* spots in neighboring domains with 71° boundaries. The reason for rarely reporting this kind of disappearance of *F* spots is that the high boundary energy greatly reduces the possibility of this type of domain wall being observed. Assuming a Maxwell–Boltzmann distribution, it can be calculated that the number of the {100} domain walls is only 14% of that of the {110} ones.[19]

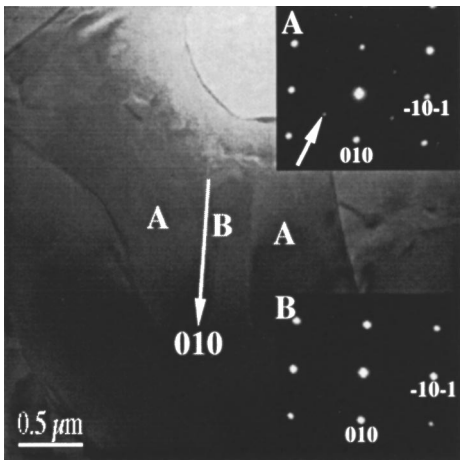

FIG. 2. 71° domain pattern viewed along $[\bar{1}01]$. Insets are SADPs of corresponding domains labeled A and B. *F* spots can be seen on the SADP of the A domain (indicated by an arrow) while no *F* spots are found in the SADP of the B domain.

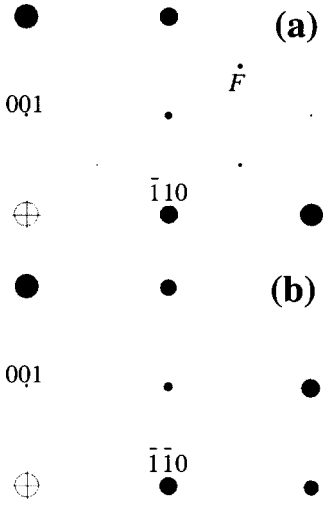

FIG. 3. Computer simulated electron diffraction pattern of PZT viewed along the ⟨110⟩ type of zone axes. For clarity, only one quarter of the pattern is shown. The zone axis is [110] for (a) and $[\bar{1}10]$ for (b).

In order to understand the relationship between the *F* spots and the domain pattern, we have conducted a computer simulation of the electron diffraction pattern by using commercial software.[20] The structural characteristics of $Pb(Zr_{0.90}Ti_{0.10})O_3$ have been studied by Glazer *et al.*[6] through neutron diffraction. The fractional coordinates were given as follows with a hexagonal cell.

	x	*y*	*z*
Pb	0	0	0.2816
Zr/Ti	0	0	0.0114
O	0.1451	0.3449	0.0833

The hexagonal lattice parameters a_h, b_h, and c_h are related to the double pseudocubic cell $2a_p \times 2b_p \times 2c_p$ by the following transformation:

$$a_h = a_p - c_p, \quad b_h = -a_p + b_p, \quad c_h = 2a_p + 2b_p + 2c_p.$$

For the calculation of the electron diffraction patterns, the double pseudocubic cell $2a_p \times 2b_p \times 2c_p$ is used. In this double cell, all the Pb and Zr/Ti atoms are displaced along the [111] direction to give a polar ferroelectric phase. The O octahedra are tilted about the [111] axis with an antiphase tilt system $a^-a^-a^-$ (in the notation of Glazer[16]). The recent neutron diffraction results are adopted in the simulation where the Pb ions are further shifted along [100] and [010] alternatively (similar to Fig. 8 of Ref. 15).

The computer simulated electron diffraction patterns along the [110] and $[\bar{1}10]$ zone axes are compared in Fig. 3. When the zone axis is [110], the *F* spots can be observed.[21] However, when the zone axis is $[\bar{1}10]$, there are no *F* spots observed. For zone axes like [101], [011], $[\bar{1}01]$, and $[0\bar{1}1]$, where the simulated diffraction patterns are not shown, the *F* spots can be observed except at positions where $h=k$. The results indicate that for this antiphase tilted system, the ⟨110⟩-type zone axes are no longer equivalent among each other. Therefore, the electron diffraction patterns observed along the ⟨110⟩-type zone axes need to be explained with

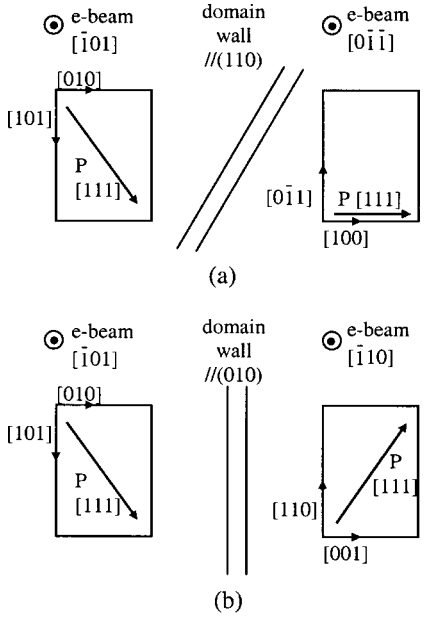

FIG. 4. Schematic drawing of the 109° (a) and 71° (b) domains. The local indexing of the domain is such as to satisfy the condition that the polarization vector (P) of the domain always pointing to the [111] direction. It should be noted that all the polarization vectors are lying in the plane of paper except the one in the right domain of (a). The electron beam is pointing out of and normal to the plane of paper.

care. There are possibilities (about 1/6) that sometimes the F spots do not appear.

Based on the above computer simulation results, the domain patterns and the corresponding electron diffraction pattern observed in Figs. 1 and 2 can be schematically explained in Fig. 4. A 109° domain viewed along $[\bar{1}01]$ is drawn in Fig. 4(a). The electron beam points perpendicularly out of the paper and the domain boundary is inclined to the electron beam. For the left domain, the electron beam is along the $[\bar{1}01]$ direction so that the F spots can be seen according to the computer simulation results. For the right domain, the same electron beam is now pointing along the $[0\bar{1}1]$ direction according to the local crystallographic orientation of that domain. In this case, the F spots can still be observed. Therefore, the F spots can be observed in neighboring domains forming a 109° boundary, as seen in Fig. 1.

Similarly, Fig. 2 can be explained based on a 71° boundary viewed along $[\bar{1}01]$, as shown in Fig. 4(b). The electron beam is again pointing out of the paper but the domain boundary is parallel to the beam in this case. For the left domain, the electron beam is along the $[\bar{1}01]$ direction so that the F spots are observed. However, for the right domain, the electron beam is now pointing along the $[\bar{1}10]$ direction following the local crystallographic orientation. In this case the F spots are forbidden. Therefore, the F spots only appear in alternative domains forming a 71° domain boundary, which is experimentally observed (Fig. 2). The alternating appearance of the F spots is rarely reported due to the fact that the 71° domain boundary is not energetically favorable.

In summary, computer simulation has shown that the F spots are forbidden at $h=k$ positions so that they do not appear in the electron diffraction pattern if viewed along the $[1\bar{1}0]$ direction. Two types of domain patterns and their corresponding electron diffraction patterns can thus be explained, i.e., the F spots are observed in the neighboring 109° domain and they disappear, in turn, in the neighboring 71° domains.

One of the authors (H.H.) is grateful for the financial support from Nanyang Technological University and The Hong Kong Polytechnic University (Grant No. G-YX09).

[1] B. Jaffe, W. R. Cook, and H. Jaffe, *Piezoelectric Ceramics* (Academic, London, 1971).
[2] B. Noheda, D. E. Cox, G. Shirane, J. A. Gonzalo, L. E. Cross, and S.-E. Park, Appl. Phys. Lett. **74**, 2059 (1999).
[3] R. Clarke, A. M. Glazer, F. W. Ainger, D. Appleby, N. J. Poole, and S. G. Porter, Ferroelectrics **11**, 359 (1976).
[4] R. W. Whatmore and A. J. Bell, Ferroelectrics **35**, 155 (1983).
[5] H. Huang, Z. Tianshu, J. T. Oh, and P. Hing, Ferroelectrics **274**, 55 (2002).
[6] A. M. Glazer, S. A. Mabud, and R. Clarke, Acta Crystallogr., Sect. B: Struct. Crystallogr. Cryst. Chem. **34**, 1060 (1978).
[7] D. Viehland, Phys. Rev. B **52**, 778 (1995).
[8] H. Huang, J. Guo, L. B. Kong, H. H. Hng, J. T. Oh, P. Hing, and O. K. Tan, Solid State Commun. **125**, 297 (2003).
[9] J. Ricote, D. L. Corker, R. W. Whatmore, S. A. Impey, A. M. Glazer, J. Dec, and K. Roleder, J. Phys.: Condens. Matter **10**, 1767 (1998).
[10] D. Viehland, J.-F. Li, X. Dai, and Z. Xu, J. Phys. Chem. Solids **57**, 1545 (1996).
[11] D. Forst, J. F. Li, Z. Xu, and D. Viehland, J. Am. Ceram. Soc. **81**, 2225 (1998).
[12] Z. Xu, D. Viehland, P. Yang, and D. A. Payne, J. Appl. Phys. **74**, 3406 (1993).
[13] E. L. Colla, I. M. Reaney, and N. Setter, J. Appl. Phys. **74**, 3414 (1993).
[14] I. M. Reaney, E. L. Colla, and N. Setter, Jpn. J. Appl. Phys., Part 1 **33**, 3984 (1994).
[15] I. M. Reaney, A. Glazounov, F. Chu, A. Bell, and N. Setter, Br. Ceram. Trans. **96**, 217 (1997).
[16] A. M. Glazer, Acta Crystallogr., Sect. A: Cryst. Phys., Diffr., Theor. Gen. Crystallogr. **31**, 756 (1975).
[17] D. L. Corker, A. M. Glazer, R. W. Whatmore, A. Stallard, and F. Fauth, J. Phys.: Condens. Matter **10**, 6251 (1998).
[18] J. Ricote, R. W. Whatmore, and D. J. Barber, J. Phys.: Condens. Matter **12**, 323 (2000).
[19] C. A. Randall, D. J. Barber, and R. W. Whatmore, J. Mater. Sci. **22**, 925 (1987).
[20] CaRIne Crystallography 3.1.
[21] Some of the simulated intensities of the F spots are low and not consistent with the experiment. This may result from many factors, such as the refined shift of Pb ions not being accurate from the neutron diffraction. Dynamical effect may also affect the intensities. In the present work we only focus on the question of whether the intensity of F spots is nonzero. Computer simulation clearly shows that the intensities of the $\frac{1}{2}\{hhl\}$ superlattice reflections are all zero.